Accepted Manuscript

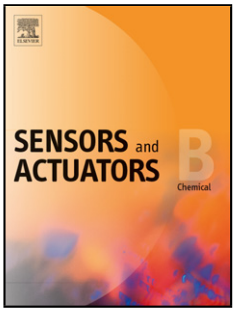

Title: Distributed feedback lasers based on perylenediimide dyes for label-free refractive index sensing

Author: Marta Morales-Vidal Pedro G. Boj José A. Quintana José M. Villalvilla Aritz Retolaza Santos Merino María A. Díaz-García

PII: S0925-4005(15)30105-2
DOI: http://dx.doi.org/doi:10.1016/j.snb.2015.07.055
Reference: SNB 18786

To appear in: *Sensors and Actuators B*

Received date: 24-3-2015
Revised date: 3-7-2015
Accepted date: 13-7-2015

Please cite this article as: M. Morales-Vidal, P.G. Boj, J.A. Quintana, J.M. Villalvilla, A. Retolaza, S. Merino, M.A. Díaz-García, Distributed feedback lasers based on perylenediimide dyes for label-free refractive index sensing, *Sensors and Actuators B: Chemical* (2015), http://dx.doi.org/10.1016/j.snb.2015.07.055

Distributed feedback lasers based on perylenediimide dyes for label-free refractive index sensing

Marta Morales-Vidal[a], Pedro G. Boj[b], José A. Quintana[b] , José M. Villalvilla[a] , Aritz Retolaza[c,d], Santos Merino[c,d] , María A. Díaz-García[a,*]

[a]Dpto. Física Aplicada, Instituto Universitario de Materiales de Alicante and Unidad Asociada UA-CSIC, Universidad de Alicante, 03080 Alicante, Spain
[b]Dpto. Óptica, Instituto Universitario de Materiales de Alicante y Unidad Asociada UA-CSIC, Universidad de Alicante, 03080 Alicante, Spain
[c]Micro and Nano Fabrication Unit, IK4-Tekniker, 20600 Eibar, Spain
[d]CIC microGUNE, 20500 Arrasate-Mondragón, Spain

[*]Corresponding author: maria.diaz@ua.es

Keywords: label-free sensors, organic lasers, distributed feedback, photostability, perylenediimides

ABSTRACT

The refractive index sensing capabilitity of distributed feedback (DFB) lasers based on highly photostable (under ambient conditions) perylenediimide-based active films, are reported. The sensor bulk sensitivity is determined from changes in the laser emission wavelength upon exposure to different liquids. The role of the active film thickness (h_f) on the sensor sensitivity and on the laser parameters is studied. Sensors based on very thin films (h_f = 160 nm) show the highest sensitivities, but their laser thresholds are relatively high and their operational durabilities moderate. The use of thicker films (h_f = 850 nm) allows reducing the laser threshold and increasing the durability by two orders of magnitude. In this case, a higher sensitivity is achieved when the sensor operates at the wavelength corresponding to the first-order TE_1 mode, instead of at the TE_0 one. Finally, it is also shown that the inclusion of a high refractive index TiO_2 layer on top of the sensor structure improves the sensitivity by around two times.

1.-Introduction

Label-free refractive index sensors are ideal devices for highly sensitive and possibly specific non-intrusive sensing with great potential in a variety of applications such as drug discovery, biological research, diagnostic tests, food safety, and environmental monitoring [1]. Over the past decades, different types of optical resonant refractive index sensors have been proposed. Most of them are based on passive optical structures such as gold films for surface plasmon resonance [2,3], photonic crystals [4-7], microrings [8], microsphere [9] and microtoroid [10] that interact with an external light source via reflection, transmission or waveguide coupling. Such sensors generally detect the resonant wavelength shift due to the interaction between the evanescent electric field of the resonant modes and the target analyte deposited on the sensor surface. The sensing performance is typically characterized by the bulk sensitivity, *Sb*, defined as the resonance wavelength change per refractive index unit (expressed in nm/RIU units). Also important is the sensor resolution, *r*, which refers to the minimum wavelength shift that can be measured. The sensor resolution and the sensor sensitivity combines to give the system limit-of-detection LOD = *r*/*Sb* in RI units [11]. In passive resonators, the strategies which allow improving the resolution generally lead to a reduction of *Sb*, establishing a trade-off for their optimization. Thus, surface plasmon polaritons on gold films have been widely used as refractometric sensors due to its high sensitivity, even though wide peak resonances dealt to no optimum LOD. Bloch Surface Waves (BSW) on dielectric one-dimensional Photonic Crystals are equivalent to surface plasmon polaritons (SPP) on thin metal films and share some common characteristics. However, since dielectrics are characterized by much lower extinction than metals, BSW resonances appear much narrower than those observed for SPP [12]. Recently, a fluorescent multi-layered dielectric structure was used for detecting spectral changes of the BSW-coupled light emission due to an external perturbation of the refractive index, obtaining high sensitivities and a LOD down to 3 x10^{-6} [13].

The second-order solid-state organic distributed feedback laser (DFB) [14,15] represents the next step from passive to active optical refractometric sensors, because the structure incorporates its own source of optical gain and feedback, so that it allows achieving narrow bandwidth output through the process of stimulated emission [16,17]. Although the linewidths achievable by DFB sensors are generally not narrower than those obtained with some of the sensors mentioned, they are simultaneously capable of high sensitivity and a high degree of resolution. In addition, DFB sensors show significant advantages for label-free sensing, including: (i) simple implementation; these sensors require neither nanometer-level precision for positioning of optical fibers or waveguides to the resonator perimeter, nor high precision tunable lasers as the illumination source [18], (ii) the platform can be fabricated through simple fabrication techniques such as interference lithography or nanoimprint lithography (NIL), enabling easily the extension to large scale production, while thin films of active materials are most commonly deposited by evaporation, spin-coating, ink-jet printing or horizontal dipping [18], and (iii) an organic laser structure can be fabricated on a mechanically flexible substrate, providing a platform easily integrated into existing assay equipment [19]. Moreover, DFB sensors meet also the requirement for multiplexing sensing and have demonstrated in some cases the possibility of using compact laser diodes or even light emitting diodes [LEDs] [20] as the optical pump, which constitutes a promising scheme for their commercialization. State-of-the-art figure-of-merit for DFBs are in the range of 7×10^{-6} RIU [21], while the lowest LODs of optical refractive index sensors are in the range of 10^{-7} to 10^{-8} RIU and the lowest limits for photonic crystal sensors are 10^{-5} RIU [1,7]. Different from DFB sensing, and sharing most of advantages pointed out above but not including a gain active medium, photonic crystal (PhC) resonant reflection was recently proposed [22, 23] to study cell dynamics, the presence of single metallic or dielectric nanoparticles on top of the PhC structure, or the use of these nanoparticles conjugated with biomolecules for the detection of specific antigens.

A wide variety of materials have been used to fabricate the active layers of DFB sensors: organic semiconductors prepared as neat films, such as truxene-core molecules [24] or semiconducting polymers [25]; or laser dyes dispersed in inert polymers, for example Rhodamine 590 in the SU-8 resist [19,26], Coumarin 503 in poly(methyl methacrylate) (PMMA) [16] or Pyrromethene 597 in Ormocore [21]. Among many families of laser dyes, pyrromethenes and perylenediimides (PDIs) are among the most photostable (independently on the type of matrix or device). There has been extensive work in the development of sophisticated matrixes including the dye covalently linked (not dispersed), in which dyes such those of the Rhodamine family, or others, can improve their photostability significantly [27]. But note that such data are obtained in monoliths pumped transversely as done with liquid laser dyes, but not in waveguide films, nor in DFB devices. Until the present study, the use of PDI-based DFB lasers as sensors has not been demonstrated. A relevant feature of DFB lasers based on PDIs dispersed in thermoplastic polymers, such as polystyrene (PS) or PMMA, as active films, is the simultaneous combination of an excellent photostability half-life under operation in ambient conditions, up to 10^5 pump pulses, and a relatively low DFB threshold of 3 kW/cm^2 [28,29], considerably better than those of DFBs based on other materials. For example, DFB sensors based on Rhodamine 590 or Coumarin 503 laser dyes dispersed in polymer matrixes have shown thresholds between 10 and 18 kW/cm^2 [16,26,30], without published photostability data. DFB sensors based on Pyrromethene 597 dispersed in Ormocore have shown photostability lifetimes of around 10^4 pump pulses and relatively high DFB thresholds (70 kW/cm^2) [21]. Worth to mention are DFB sensors based on truxene-core molecules, showing a reasonable combination of threshold (12 kW/cm2) and operational lifetime (around 10^3 pump pulses) [24,31]. Another remarkable property of PDI-doped PS materials is their excellent thermal and chemical stability, which enables grating imprinting by thermal-NIL directly onto the active film and consequently in a very simple and economical way [32].

It is known that the sensitivity of a DFB sensor is larger when the active film thickness is as thin as possible [17,21,33]. However, a problem of using a very thin active film in the DFB laser is that its threshold increases due to its lower absorption and therefore emitted light intensity, and also due to a poor confinement of the waveguide mode [34]. Also the operational lifetime would decrease, given that the device needs more pump intensity to operate [28,35]. While strategies towards sensitivity improvement have been previously explored, less attention has been devoted to the effect of these strategies on the device laser threshold and operational lifetime. Both parameters are important to develop simple, scalable fabrication of organic lasers operating as sensors that may be compatible with inexpensive pump sources and therefore provide a compact, inexpensive approach to integrated visible lasers operating as sensors [20]. An interesting approach in this context is the use of a resonant optical pumping scheme for the DFB, consisting in coupling the excitation light into a distinct resonant mode of the laser cavity through illumination at a specific incident angle. This approximation has demonstrated success in reducing the laser pump threshold, and consequently also in increasing the operational lifetime, in two- and one-dimensional DFB sensors [36,37]. Another reported strategy to increase the DFB sensor sensitivity consists in depositing high refractive index layers on top of the active film [19,21,26].

Here we report DFB sensors based on highly photostable PDI-doped PS active films showing sensitivity values comparable to those obtained with other DFB sensors previously reported, while their operational durability is much superior. The role of the active film thickness (h_f) on the laser parameters (emission wavelength, threshold and operational durability) and on the sensor sensitivity is studied. Firstly, we analyze DFB sensors based on thin active films (160 nm), whose emission is associated to the TE_0 waveguide mode, aiming to optimize the sensitivity. Then, results for devices with thicker films (around 850 nm), with optimized lasing threshold and operational durability are presented. The interpretation of the DFB threshold dependence on film thickness is done in combination with amplified spontaneous emission (ASE) studies in films without gratings. Finally, the effect on the sensor performance of depositing a high refractive index TiO_2 layer on top of the devices is also explored.

2.-Materials and methods

2.1 Device structure and operation principle

The structure of the simplest device (see Fig. 1a), denoted here as single-layer DFB laser, consists of a planar asymmetric waveguide consisting of a PDI-doped PS film with thickness h_f and refractive index $n_f = 1.59$ (at $\lambda = 580$ nm), deposited over a transparent fused silica substrate ($n_s = 1.46$, at $\lambda = 580$ nm) patterned with a periodic one-dimensional DFB grating (overall size: 2 mm × 2 mm; period: $\Lambda = 376$ nm; depth: $d = 60$ nm). The DFB grating was engraved by thermal-NIL and subsequent etching, prior to active film deposition, as described below. Devices including an additional top TiO_2 layer (thickness $h_t = 26$ nm; refractive index $n_t = 2.4$, at $\lambda = 580$ nm), see Fig. 1b, denoted as two-layer DFB lasers, were also prepared. For ASE studies, samples consisting of active films deposited over bare fused silica (without gratings) were used. From previous film thickness dependence studies of the waveguide, ASE and DFB performance of PDI-doped PS films [34,38], it is known that the observed DFB laser peaks correspond to TE waveguide modes, and not to transverse magnetic (TM) ones. Lasing associated to TM modes occurs at a much higher threshold, so in order to be observed, devices would need to be pumped at larger intensities. The TE character to the DFB emission was verified by means of a polarizer.

The DFB laser sensor works, according to the Bragg condition, as an optical cavity and emits light through stimulated emission upon the absorption of input energy. The emission wavelength (λ_{DFB}) is close to the wavelength at which the cavity resonates (λ_{Bragg}), which is determined by the grating period (Λ), the diffraction order (m) and the effective refractive index (n_{eff}), according to the expression:

$\lambda_{\mathrm{Bragg}} = (2\, n_{\mathrm{eff}}\, \Lambda)/m$ (1)

The n_{eff} parameter depends on n_s, n_f, h_f and the refractive index of the cover layer (air in the case of the devices without TiO_2 layer). The DFB structure provides both, the feedback mechanism and the out-coupling for the laser. Using a second-order Bragg grating (m = 2 in Eq. 1), light is emitted perpendicularly to the active film by first-order diffraction. The grating period value of our devices (Λ = 376 nm) was chosen in order to obtain operation in the second order, at wavelengths in the range 545-595 nm, at which the PDI photoluminescence (PL) is sufficiently efficient and there is no strong self-absorption for the various film thickness used.

The deposition of superstrates of different refractive index on top of the DFB device results in changes in the laser wavelength, due to changes in n_{eff}, which constitutes the operational principle of the sensor. In this work the DFB sensors have been exposed to liquid superstrates of different refractive index, n: distilled water, aqueous solutions of glycerin (25, 50, and 75%) and pure glycerin. The bulk refractive index sensitivity, *Sb*, determined as the derivative of the lasing wavelength shift, $\Delta\lambda$, with respect to n, has been determined in the biological range (at n = 1.33).

INSERT FIG. 1

2.2 Device fabrication.

For DFB grating preparation, a transparent fused silica master with a one-dimensional DFB grating of periodicity Λ = 376 nm, equal line and space and a depth d = 100 nm, fabricated by e-beam lithography and reactive ion etching (NIL Technology), was used. The DFB grating was surrounded by concentric rectangles to maintain a constant residual layer thickness. The stamp was treated with tridecafluoro-(1,1,2,2)-tetra-hydrooctyl-trichlorosilane antiadhesive coating deposited from the vapor phase [39]. This treatment is very important to decrease the surface energy of the masters and, therefore, to facilitate the demolding step. A layer of 100 nm thickness of mr-I7010R (from Microresist Technology GmbH) was spin-coated on a 4-inch transparent fused silica wafer. The NIL (or hot-embossing) process was carried out in a Jenoptik HEX03 press under vacuum at 135ºC and 10 kN force during 12 minutes. The demolding temperature was 40ºC. After demolding, a residual layer of 50 nm was obtained. This residual layer was removed under an O_2 plasma (10 sccm, 75 mTorr, 20W) and the grating was transferred to the fused silica wafer by CHF_3/Ar plasma etching (25 sccm CHF_3, 25 sccm Ar, 30 mTorr, 200W). Both etching processes were carried out in an Oxford PlasmaLab ICP 80+. A scanning electron microscope micrograph of one of the obtained gratings is supplied in the supporting information (Fig. S1).

In the two-layer DFB devices, the TiO_2 layer was prepared in a MIDAS 450 semi-industrial vacuum chamber designed by IK4-TEKNIKER. This chamber includes a closed field unbalanced magnetron sputtering system with three rectangular evaporators (500 mm x 125 mm). A metal Ti target (99.6% purity) was reactively sputtered in Ar + O_2 atmosphere by pulsed DC magnetron sputtering technology (Pinnacle® Plus+, AE). The Ar flow was kept constant at 40 sccm, while the O_2 flow was controlled via Speedflo controller (Gencoa) in order to hold the process in high rate metallic or transition mode. The required voltage for this mode was set at 330V and the average power was 3kW.

Active films were prepared by spin-coating a toluene solution containing PS, as inert matrix polymer, and 1.0 wt% (with respect to PS) of perylene orange (PDI-O, chemical structure in Fig. 1(c)), on top of a substrate. In the case of the single-layer devices, fused silica substrates with the engraved DFB gratings were used. The two-layer devices were prepared depositing TiO_2 layers on top of the single-layer systems. After deposition, active films were heated at 90º C for 120 min to eliminate the residual solvent. PS (M_w = 35000 g/mol) and toluene was purchased from Sigma-Aldrich. PDI-O (purity higher than 99.5%) was purchased from Phiton. The percentage of polymer with respect to the solvent was adjusted in order to obtain h_f values between 160 and 850 nm, depending on the device. Film thickness was determined by the fringe pattern of the absorption spectrum, measured by a Jasco V-650 UV-VIS spectrophotometer.

2.3 Optical characterization

Standard PL measurements were carried out in a Jasco FP-6500 fluorimeter. DFB emission characterization was performed under excitation with a pulsed Nd:YAG (YAG-yttrium aluminium garnet) laser (5.5 ns, 10 Hz) operating at 532 nm. The pump beam over the sample (elliptical with a minor axis of 1.1 mm) was incident at an angle of around 20° with respect to the normal to the film plane. The small deviation from normal incidence aimed to facilitate light collection, by means of an Ocean Optics MAYA2000 fiber spectrometer, in a direction perpendicular to the sample surface. The nominal wavelength resolution of this spectrometer is 0.07 nm. However, since the measured spectrum is formed by discrete points separated by steps of 0.035 nm, the peak wavelength can be estimated with a resolution better than that of the spectrometer by fitting the experimental results to a Lorentzian curve [26] or using a center of mass model approach [21]. In those cases, the sensor resolution is defined to be twice the standard deviation of a set of successive measurements and its value is usually of the order of one picometer. The excitation and collection geometry (see Fig. 1(a)) differs slightly from the one used in previous works to characterize PDI-based DFB lasers [35], since here excitation and light emission collection is done through the substrate, with the sample placed horizontally with respect to the optical table to facilitate the deposition of liquid superstrates. This geometry, which requires the use of a transparent substrate, avoids disturbing the analyte with the pump beam.

The characterization of the ASE properties of the PDI-doped PS films over substrates without gratings was done in the standard setup used in previous works for such purpose [29,38]. The excitation beam is the same one used for DFB studies, but here a cylindrical lens and an adjustable slit were used to shape the beam into a stripe of 3.5 mm by 0.50 mm, which was incident directly upon the active film in a perpendicular direction. The stripe was placed right up to the edge of the film, from where PL emission was collected with an Ocean Optics USB2000-UV-VIS fiber spectrometer with 600 grating lines and a resolution in determining the emission linewidth of 1.3 nm. The precision in measuring the emission wavelength was around half of this value.

3.-Results and discussion

3.1.-Single-layer DFB laser sensors: PDI-O-doped PS over resonator

We first prepared a DFB sensor with a very thin active film (h_f = 160 nm), with the aim of obtaining the largest possible sensor sensitivity. The sensitivity increases as h_f diminishes because the slope of the n_{eff} (and consequently that of λ_{Bragg} , see eq. (1)) versus h_f curve increases. This concept is illustrated in Fig. S2 in the SI section, which displays λ_{Bragg} as a function of h_f for a device exposed to air and water. The n_{eff} values used for the calculation of λ_{Bragg} have been obtained by solving the propagation wave equation for the simplest possible model waveguide, consisting of a film of thickness h_f deposited over a planar fused silica substrate of infinite thickness [38,40]. It has also assumed that the cover layer (air or water) has infinite thickness. The calculated cut-off thickness for the waveguide in air for the TE_0 and TE_1 modes are respectively $h_{cut-off}$ (TE_0) = 149 nm and $h_{cut-off}$ (TE_1) = 600 nm. So, the election of h_f = 160 nm aimed to be just above $h_{cut-off}(TE_0)$. The refractive index sensing capability of this sensor with h_f = 160 nm is illustrated in Figure 2, which shows the experimental DFB spectra in air and after the deposition of liquids of different refractive index on top of the device. The wavelength shift upon water deposition ($\Delta\lambda_{A-W}$) is 4.2 nm. The sensor sensitivity near the refractive index value of 1.33 (the biological range) is *Sb* = 32 nm/RIU (see Fig. 2, inset). This *Sb* value is comparable to those reported for other single-layer waveguide DFB sensors (*Sb* = 20 nm/RIU at n = 1.33) [16,24], which have demonstrated their capability to detect biomolecules [16,41]. This indicates that our PDI-O-based DFB sensors have sufficient sensitivity to be used for biomolecule detection. Importantly, these sensitivities can be further improved by including high index top layers (see section 3.2) or by increasing the refractive index difference between active film and substrate, as recently demonstrated [25]. The sensor resolution was calculated by analyzing with the center mass model [21] the peak corresponding to the case of water superstrate. Thus, from a set of 50 spectra, we determined a resolution of 0.8 pm and a LOD of 2.5×10^{-5} RIU. This LOD value is similar to that of photonic crystal sensors [7, 42].

INSERT FIGURE 2

As previously mentioned, a drawback of using a very thin active film is that the DFB threshold becomes larger and the operational lifetime lower than those achievable with DFBs based on thicker films [28,34]. In order to improve the DFB threshold and operational lifetime, we have prepared devices with thicker active films. First, we fabricated a laser with h_f = 180 nm, only slightly thicker than the one just discussed. The aim was to test how critical a change of thickness is in the sensor sensitivity and its threshold. Following the same procedure shown in the inset of Fig. 2, the sensor sensitivity in the biological range is *Sb* = 28 nm/RIU, only slightly inferior, while its threshold improves considerably, as discussed in detail below.

The strategy followed here to obtain a device with optimized threshold and operational durability, while keeping a reasonable sensitivity, has been to prepare an even thicker film, particularly h_f = 850 nm, which supports two waveguide modes (TE_0 and TE_1). The idea is to make the DFB device operating at a wavelength associated to the TE_1 mode, whose dispersion curve for thick films has a larger slope than that of the TE_0 one (see Fig. S2), and therefore with better sensitivity. The effect on the DFB spectra and the thresholds of changing h_f is analysed through Figure 3, which shows results for the three prepared devices (with h_f values of 160, 180 and 850 nm). Data for the ASE spectra and thresholds of films of the same characteristics, but deposited over substrates without gratings are also provided. The interest of studying also the ASE properties relies on the fact that the ASE wavelength practically does not change when h_f is varied, in contrast to the DFB wavelength, which is very sensitive to changes in h_f. So, ASE analysis constitutes a useful tool to clarify the role of the waveguide mode confinement on the threshold [38]. As observed in Fig. 3(a), the ASE spectrum red-shifts only slightly when film thickness increases, while the ASE threshold increases considerably ca. from 6 kW/cm^2 (for h_f = 850 nm) up to 120 kW/cm^2 when h_f is decreased down 160 nm (see Fig. 3(b)). This is due to the lower absorption of the latter, and therefore PL intensity, as well as to a poorer confinement of the waveguide mode [43]. The ASE photostability of the thin film is inferior to that of the thick film. Indeed, the very large ASE photostability half-life value of 2×10^5 pump pulses (under excitation two times above the ASE threshold) of the 850 nm-thick film decreases by around one order of magnitude in the thinnest film. But this difference is not a material property dependent on film thickness, but a direct consequence of the higher threshold of the thin film, which requires a higher pumping intensity for operation and this parameter affects critically the photostability performance [28,35].

In the case of the DFB lasers, changes in h_f have an important effect on λ_{DFB} (see Fig. 3(c)) due to the DFB grating. Thus, the analysis of the effect of changing h_f on the threshold, which is also quite drastic (see Fig. 3(d)) is more complex than in the ASE case. Devices with the thinnest films (h_f = 160 nm and h_f = 180 nm) show one single peak, associated with the TE_0 mode. Their thresholds are quite large (210 and 73 kW/cm^2, respectively) mainly because they emit far from the wavelength of maximum gain (given by the ASE wavelength), but it is also because waveguide mode confinement is poor, as previously shown by the ASE data. The important role of the waveguide mode confinement is confirmed by the fact that for the film with h_f = 850 nm, the threshold of the DFB peak associated to the TE_0 mode is only 20 kW/cm^2, although this one also emits at a wavelength far from the peak gain. Importantly, the lowest threshold was obtained for this thicker film, but for the DFB peak associated with TE_1 mode (3 kW/cm^2), due to its proximity to the peak gain. With regards to the DFB operational durability, results are in accordance with previously discussed ASE photostability performance. The DFB laser based on the thick active film shows an operational half-life of around 10^5 pump pulses (under excitation two times above the DFB threshold), one order of magnitude larger than that of the thinnest film. The reduction of lifetime in this latter device is due to the need of pumping with a higher intensity, due to its higher threshold.

INSERT FIGURE 3

The sensitivity of the device with h_f = 850 nm upon deposition of different liquids was determined for both DFB peaks (see Figure 4). Upon water deposition, the wavelength shift for the TE_1 mode is $\Delta\lambda_{A\text{-}W}$ = 1.3 nm, two times larger than that obtained with the TE_0 mode ($\Delta\lambda_{A\text{-}W}$ = 0.6 nm). The advantage of using the TE_1 mode is also reflected in its higher sensitivity value (Fig. 4, inset). Note that although this *Sb* value is smaller than that of devices based on thin films, its threshold is significantly lower and its operational lifetime is significantly larger. This result is important because for certain applications, not requiring a very large sensitivity, but a low threshold and long device lifetime, the use of thick films would be a wise option.

INSERT FIGURE 4

3.2.- Two-layer DFB laser sensors: TiO_2/PDI-O-doped PS over resonator

Here we study the effect of having a top layer of high refractive index in the DFB device, because this has demonstrated success for increasing the sensitivity of other DFB sensors reported [19,21,26]. We first analyze this in sensors based on thin active films (h_f = 160 nm), including a top TiO_2 layer, see Figure 5(a). First of all, it should be noted that λ_{DFB} appears at a value of around 10 nm above the one obtained with the device without TiO_2 layer (see Fig. 2). The shift in the emission wavelength upon water deposition is now $\Delta\lambda_{A\text{-}W}$ = 10.2 nm and the sensitivity *Sb* = 60 nm/RIU. These values are around two times larger than those obtained with devices without TiO_2. This *Sb* value is comparable to that reported by Vannahme et al. [21] (*Sb* = 70 nm/RIU, at n = 1.33) which performed a detailed investigation to optimize the thickness of the TiO_2 layer to obtain the maximum sensitivity. The DFB spectra consisted in a single peak associated with the TE_0 mode, except in the case of glycerin exposure which showed an additional peak corresponding to the TE_1 mode. The association of a given laser peak to a certain waveguide mode was done as in previous section through Eq. (1), although in this case the effective indexes could not be calculated in the frame of a waveguide film between two media of infinite thickness, given that the thickness of the TiO_2 layer is only 26 nm. Instead, a multilayer model was used [43].

INSERT FIGURE 5

The effect of including a top TiO_2 layer in the sensor structure has also been investigated for DFBs based on thick active films, which as discussed in previous section are particularly interesting for their lower thresholds and higher operational durabilities. The DFB spectrum of such a device with h_f = 850 nm and the TiO_2 layer consists of several peaks associated with different waveguide modes (TE_1 and TE_2 in air; TE_1, TE_2 and TE_3 in water, etc.; see Fig. S3 in supporting information), which makes the sensing capability analysis rather complicated. Only the TE_2 mode allows sensing ($\Delta\lambda_{A\text{-}W}$ = 2.5 nm and *Sb* = 16 nm/RIU) in the same range of refractive indexes used in previous devices studied in this work, Figure 5(b), since it is the one appearing in all cases (in air, water, etc.). In accordance with the device based on a thin active film, the sensitivity also increases thanks to the inclusion of the TiO_2 layer. Nevertheless, taking into account the existence of various DFB peaks due to the multimode character of these devices, limits the interest of these devices in comparison to the ones showing only one DFB peak.

With regards to the effect on the laser threshold of the presence of the TiO_2 layer, it was observed that it becomes around two times larger than those of devices without TiO_2. This can be attributed to the presence of higher order modes, although a detailed interpretation of this issue is not an obvious task, since it depends on various parameters as already discussed.

Conclusions

DFB lasers with active films consisting of PS doped with PDI-O, showing an excellent photostability under operation in ambient conditions and a relatively low threshold, have been fabricated. Their feasibility as bulk refractive index sensors has been investigated through the changes observed in their laser emission wavelength upon exposure to different liquid superstrates: distilled water, aqueous solutions of glycerin (25, 50, and 75%) and pure glycerin. The role of the active film thickness (h_f) on the laser parameters (emission wavelength, threshold and operational durability) and on the sensor sensitivity has been studied. The device based on a very thin film of h_f = 160 nm has shown in the biological range a sensitivity of Sb = 32 nm/RIU, comparable to other single-layer DFB sensors reported in the literature, while its threshold is relatively high (I_{th}^{DFB} = 200 kW/cm^2) and its operational durability moderate (half-life of around 10^4 pump pulses). In this case, the sensor resolution calculated from a set of 50 spectra using the center mass model approach is 0.8 pm, which leads to a LOD of 2.5×10^{-5} RIU. A slight increase of h_f up to only 180 nm has allowed decreasing the threshold by three times, while its sensitivity diminishes only slightly (Sb = 28 nm/RIU). The increase of h_f up to around 850 nm allows improving considerably both, the laser threshold and the operational durability, although the sensitivity decreases. In this case the overall performance is better (by several times) when the sensor operates at the wavelength corresponding to the first-order TE_1 mode (I_{th}^{DFB} = 3 kW/cm^2, half-life 10^5 pump pulses, Sb = 7.6 nm/RIU). Finally, the inclusion of a high refractive index TiO_2 layer on top of the sensor structure improves the sensitivity by around two times, although in the case of devices based on thick films, the sensor operation is complicated by the appearance of many peaks associated with high order waveguide modes.

Acknowledgements

This work was supported by the Spanish Government (MINECO) and the European Community (FEDER) through grant no. MAT-2011–28167-C02. This work was partially funded by the Basque Government within the framework of the Etortek Program (Grant No. IE13-360). M.M. has been partly supported by a MINECO FPI fellowship (no. BES-2009-020747).

References

[1] X. Fan, I.M. White, S.I. Shopova, H. Zhu, J.D. Suter, Y. Sun, Sensitive optical biosensors for unlabeled targets: A review, Anal. Chim. Acta 620 (2008) 8-26.

[2] J. Homola, S.S. Yee, G. Gauglitz, Surface plasmon resonance sensors: review, Sens. Actuators B 54 (1999) 3-15.

[3] V. Koubová, E. Brynda, L. Karasová, J. Škvor, J. Homola, J. Dostálek, P. Tobiška, J. Rošický, Detection of foodborne pathogens using surface plasmon resonance biosensors, Sens. Actuators B 74 (2001) 100-105.

[4] B.T. Cunningham, P. Li, S. Schulz, B. Lin, C. Baird, J. Gerstenmaier, C. Genick, F. Wang, E. Fine, L. Laing, Label-free assays on the BIND system, J. Biomol. Screen. 9 (2004) 481-490.

[5] M. Kristensen, A. Krüger, N. Groothoff, J. García-Rupérez, V. Toccafondo, J. García-Castelló, M.J. Bañuls, S. Peransi-LLopis, A. Maquieira, Photonic crystal biosensor chip for label-free detection of bacteria, Optical Sensors, Optical Society of America (2011) SWB1.

[6] S.M. Shamah, B.T. Cunningham, Label-free cell-based assays using photonic crystal optical biosensors, Analyst 136 (2011) 1090-1102.

[7] B. Cunningham, P. Li, B. Lin, J. Pepper, Colorimetric resonnat reflection as a direct biochemical assay technique, Sens. Actuators B 81 (2002) 316-328.

[8] A.L. Washburn, L.C. Gunn, R.C. Bailey, Label-free quantitation of a cancer biomarker in complex media using silicon photonic microring resonators, Anal. Chem. 81 (2009) 9499-9506.

[9] I.D.W. Samuel, G.A. Turnbull, Organic semiconductor lasers, Chem. Rev. 107 (2007) 1272-1295.

[10] A.M. Armani, R.P. Kulkarni, S.E. Fraser, R.C. Flagan, K.J. Vahala, Label-free, single-molecule detection with optical microcavities, Science 317 (2007) 783-787.

[11] I.M. White, X. Fan, On the performance quantification of resonant refractive index sensors, Opt. Express 16 (2008) 1020–1028.

[12] W.L. Barnes, Surface plasmon-polariton length scales: a route to sub-wavelength optics, J. Opt. A, Pure Appl. Opt. 8 (2006) S87–S93.

[13] E. Descrovi, F. Frascella, M. Ballarini, V. Moi, A. Lamberti, F. Michelotti, F. Giorgis, C.F. Pirri, Surface label-free sensing by means of a fluorescent multilayered photonic structure, Appl. Phys. Lett. 101 (2012) 131105.

[14] S. Chénais, S. Forget, Recent advances in solid-state organic lasers, Polym. Int. 61 (2012) 390-406.

[15] C. Grivas, M. Pollnau, Organic solid-state integrated amplifiers and lasers, Laser Photonics Rev. 6 (4) (2012) 419-462.

[16] M. Lu, S.S. Choi, C.J. Wagner, J.G. Eden, B.T. Cunningham, Label free biosensor incorporating a replica-molded, vertically emitting distributed feedback laser, Appl. Phys. Lett. 92 (2008) 261502.

[17] C. Ge, M. Lu, W. Zhang, B.T. Cunningham, Distributed feedback laser biosensor incorporating a titanium dioxide nanorod surface, Appl. Phys. Lett. 96 (2010) 163702.

[18] C. Ge, M. Lu, X. Jian, Y. Tan, B.T. Cunningham, large-area organic distributed feedback laser fabricated by nanoreplica moulding and horizontal dipping, Opt. Express 18 (2010) 12980-12991.

[19] Y. Tan, C. Ge, A. Chu, M. Lu, W. Goldshlag, C.S. Huang, A. Pokhriyal, S. George, B.T. Cunningham, Plastic-based distributed feedback laser biosensors in microplate format, IEEE Sens. J. 12 (2012) 1174-1180.

[20] G. Tsiminis, Y. Wang, A.L. Kanibolotsky, A.R. Inigo, P.J. Skabara, I.D.W. Samuel, G.A. Turnbull, Nanoimprinted organic semiconductor laser pumped by a light-emitting diode, Adv. Mater. 25 (2013) 2826-2830.

[21] C. Vannahme, M.C. Leung, F. Richter, C.L.C. Smith, P.G. Hermannsson, A. Kristensen, Nanoimprinted distributed feedback lasers comprising TiO_2 thin films: design guidelines for high performance sensing, Laser Photonics Rev. 7 (2013) 1036-1042.

[22] W. Chen, K. D. Long, M. Lu, V. Chaudhery, H. Yu, J. S. Choi, J. Polans, Y. Zhuo, B. A.Harley and B. T. Cunningham, Photonic crystal enhanced microscopy for imaging of live cell adhesion, Analyst 138 (2013) 5886–5894.

[23] Y. Zhuo, H. Hu, W. Chen, M. Lu, L. Tian, H. Yu, K. D. Long, E. Chow, W.P. King, S. Singamaneni, B.T. Cunningham, Single nanoparticle detection using photonic crystal enhanced microscopy, Analyst 139 (2014) 1007-1015.

[24] A.M. Haughey, B. Guilhabert, A.L. Kanibolotsky, P.J. Skabara, G.A. Burley, M.D. Dawson, N. Laurand, An organic semiconductor laser based on star-shaped truxene-core oligomers for refractive index sensing, Sens. Actuators B: Chem. 185 (2013) 132-139.

[25] E. Heydari, J. Buller, E. Wischerchoff, A. Laschewsky, S. Döring, J. Stumpe, Label-free biosensor based on all-polymer DFB laser, Adv. Opt. Mater. 2 (2014) 137-141.

[26] M. Lu, S.S. Choi, U. Irfan, B.T. Cunningham, Plastic distributed feedback laser biosensor, Appl. Phys. Lett. 93 (2008) 111113.

[27] I. Garcia-Moreno, A. Costela, V. Martin, M. Pintado-Sierra, R. Sastre, Materials for a reliable solid-state dye laser at the red spectral edge, Adv. Funct. Mater. 19 (2009) 2547–2552.

[28] V. Navarro-Fuster, E.M. Calzado, P.G. Boj, J.A. Quintana, J.M. Villalvilla, M.A. Díaz-García, V. Trabadelo, A. Juarros, A. Retolaza, S. Merino, Highly photostable organic distributed feedback laser emitting at 573 nm, Appl. Phys. Lett. 97 (2010) 171104.

[29] M.G. Ramírez, M. Morales-Vidal, V. Navarro-Fuster, P.G. Boj, J.A Quintana, J.M. Villalvilla, A. Retolaza, S. Merino, M.A. Díaz-García, Improved performance of perylenediimide-based lasers, J. Mater. Chem. C 1 (2013) 1182-1191.

[30] Y. Tan, A. Chu, M. Lu, B.T. Cunningham, Distributed feedback laser biosensor noise reduction, IEEE Sens. J. 13 (5) (2013) 1972-1978.

[31] C. Foucher, B. Guilabert, A.L. Kanibolotsky, P.J. Skabara, N. Laurand, M.D. Dawson, Highly-photostable and mechanically flexible all-organic semiconductor lasers, Opt. Mater. Express 3 (5) (2013) 584-597.

[32] M.G. Ramírez, P.G. Boj, V. Navarro-Fuster, I. Vragovic, J.M. Villalvilla, I. Alonso, V. Trabadelo, S. Merino, M.A. Díaz-García, Efficient organic distributed feedback lasers with imprinted active films, Opt. Express 19 (23) (2011) 22443-22454.

[33] M. Lu, Label-free biosensor based upon replica-molded vertically emitting distributed feedback laser, Ph. D. Thesis, Graduate College of the University of Illinois, Urbana-Champaign, 2009.

[34] V. Navarro-Fuster, I. Vragovic, E.M. Calzado, P.G. Boj, J.A. Quintana, J.M. Villalvilla, A. Retolaza, A. Juarros, D. Otaduy, S. Merino, M.A. Díaz-García, Film thickness and grating depth variation in organic second-order distributed feedback lasers, J. Appl. Phys. 112 (2012) 043104.

[35] E.M. Calzado, J.M. Villalvilla, P.G. Boj, J.A. Quintana, V. Navarro-Fuster, A. Retolaza, S. Merino, M.A. Díaz-García, Influence of the excitation area on the thresholds of organic second-order distributed feedback lasers, Appl. Phys. Lett. 101 (2012) 223303.

[36] M.B. Christiansen, A. Kristensen, S. Xiao, N. A. Mortensen, Photonic integration in k-space: Enhancing the performance of photonic crystal dye lasers, Appl. Phys. Lett. 93 (2008) 231101.

[37] E.M.C. Ge, M. Lu, Y. Tan, B.T. Cunningham, Enhancement of pump efficiency of a visible wavelength organic distributed feedback laser by resonant optical pumping, Opt. Express 19 (2011) 5086-5092.

[38] E.M. Calzado, M.G. Ramírez, P.G. Boj, M.A. Díaz-García, Thickness dependence of amplified spontaneous emission in low-absorbing organic waveguides, Appl. Opt. 51 (16) (2012) 3287-3293.

[39] http://www.nilt.com/

[40] C.L. Chen, Foundations for guided-wave optics, Wiley, New Jersey, 2006.

[41] A.M. Haughey, B. Guilhabert, A.L. Kanibolotsky, P.J. Skabara, M.D. Dawson, G.A. Burley, N. Laurand, An oligofluorene truxene based distributed feedback laser for biosensing applications, Biosens. Bioelectron. 54 (2014) 679-686.

[42] S. Mandal, D. Erickson, Nanoscale optofluidic sensor arrays, Opt. Express 16 (2008) 1623-1631

[43] C. Vannahme, C.L.C. Smith, M.B. Christiansen, A. Kristensen, Emission wavelength of multilayer distributed feedback dye lasers, Appl. Phys. Lett. 101, (2012) 151123.

Figure Captions

Figure 1. Schemes of single-layer (a) and two-layer (b) DFB sensors, including excitation and collection geometry, and laser dye chemical structure (c). The single-layer sensor consists of an active layer of polystyrene doped with 1 wt% of the laser dye perylene orange, deposited over a fused silica substrate with a DFB grating as periodic nanostructure. The two-layer sensor is like the single-layer one, but covered with a TiO_2 layer. The analyte (superstrate) is a drop of liquid solution deposited on top of the device.

Figure 2. Laser spectra of a single-layer DFB sensor with h_f = 160 nm exposed to air and different liquids. Spectra (output DFB intensity, I_{out}^{DFB}, versus emission wavelength, λ from left to right correspond to air (A), water (W), and several aqueous solutions of glycerin –25 wt% (G_{25}), 50 wt% (G_{50}), 75 wt% (G_{75}) and pure glycerin (G_{100}) – on top of the device; Inset: Wavelength shift ($\Delta\lambda$) versus superstrate refractive index (n) and sensor sensitivity (Sb) determined in the biological range.

Figure 3. ASE and DFB properties for single-layer DFB sensors with different h_f values. Emission spectra and output intensity versus pump intensity curves for threshold determination are shown in (a) and (b) respectively, for ASE; and in (c) and (d) for DFB. Data shown correspond to h_f = 160 nm (A: green line, circles), h_f = 180 nm (B: red line, triangles) and h_f = 850 nm (C: black line, squares), deposited over fused silica without and with gratings, for ASE and DFB, respectively. The corresponding PL spectra are also shown (dashed blue line).

Figure 4. Laser spectra of a single-layer DFB sensor with h_f = 850 nm exposed to air and different liquids. Spectra shown correspond to air (A), water (W), and several aqueous solutions of glycerin –25 wt% (G_{25}), 50 wt% (G_{50}), 75 wt% (G_{75}) and pure glycerin (G_{100}) – on top of the device. Each DFB spectrum consists of two peaks corresponding to the TE_1 and TE_0 waveguide modes; Inset: Wavelength shift ($\Delta\lambda$) versus superstrate refractive index (n) and sensor sensitivity (Sb) determined in the biological range.

Figure 5. Laser spectra of two-layer DFB sensors (with top TiO_2 layer) exposed to air and different liquids. Spectra shown correspond to devices with h_f = 160 nm (a) and h_f = 850 nm (b) exposed to air (A), water (W), an aqueous solutions of glycerin at 50 wt% (G_{50}) and pure glycerin (G_{100}). Spectra shown in (a) correspond to TE_0 waveguide modes. The spectrum for G_{100} shows also a peak at 570 nm (not shown) associated to the TE_1 waveguide mode. Spectra shown in (b) correspond to TE_2 waveguide modes (peaks associated with other modes not shown). The wavelength shift ($\Delta\lambda$) for the laser peak associated to the TE_0 mode and TE_2 mode (insets in (a) and (b), respectively) is plotted versus superstrate refractive index (n) for sensor sensitivity (Sb) determination in the biological range.

HIGHLIGHTS

- Label-free refractive index sensors based on photostable distributed feedback lasers.
- Role of active film thickness on sensor sensitivity and on laser parameters studied.
- High sensitivity and operational durability of 180 nm-thick film laser sensor.
- Thick active films (ca. 850 nm) improve laser threshold and photostability.
- Operation at the TE_1 waveguide mode improves sensitivity of thick film-based sensors.

Biographies

Marta Morales-Vidal received the Optics and Optometry degree in 2007, the Optometry and Vision Sciences Master’s degree in 2009, and the Molecular Nanoscience and Nanotechnology Master’s degree in 2012, all of them from Alicante University (UA). She is currently working towards a PhD in Nanoscience and Nanotechnology in the UA in the “Organic electronics and photonics” group, with particular emphasis in the study of novel organic materials for lasing and the application of organic distributed feedback lasers for biosensing applications.

Pedro G. Boj obtained the PhD in physics in 1986 in the University of Valencia, in the area of optics in holographic recording materials and holographic optical elements. In 1982 he joined the Holographic Centre of the University of Alicante (UA). In 1985 he became Associate Professor of Optics at the UA, position that holds at present. His research activity evolved from the field of holography to the area of organic solid-state lasers, since 2002, when he joined the group of “Organic Electronics and Photonics” at the UA.

José M. Villalvilla graduated in Chemistry in 1985 in the Autonomous University of Madrid and received the PhD in physics in 1992 from the University of Alicante (UA), working in the area of dry recording in III-V materials with ionic beams**.** After postdoctoral work in Cambridge University, UK, during 1996, he became Associate Professor of Applied Physics at the UA, position that holds at present. In 2002 he joined the group of “Organic Electronics and Photonics”. Since then, his research activity has focussed on photoconductive polymers and on the fabrication of organic distributed feedback lasers by holographic lithography.

José A Quintana received the Ph.D. degree in Optics from the University of Alicante (UA), Spain, in 1975. As Associate Professor he taught Solid-state Physics at the University of Valencia, Spain, from 1968 until 1972, and Physics and Optics at the UA, from 1973 until 2008.

He conducted research in the area of holography from 1968 until 2000. He joined the “Organic Electronics and Photonics” group at the UA in 2004 and since then, he works in the area of Organic Electronics.

Aritz Retolaza received the Chemistry Science degree in 1999 and the Ph.D. degree in thermal and mechanical properties of polymer blends, in 2004, both from the University of the Basque Country (Spain). Since 2005 he has worked in the Micro and Nanofabrication Unit of IK4-Tekniker, developing UV-lithography and NIL technologies. He has studied basic aspects of NIL, such as bending, demoulding and lift-off after imprinting, and he has applied this technology in different fields such as organic lasers, DNA manipulation in nanofluidic chips, effect of micropatterned surfaces on cell morphology and localized surface Plasmon resonance.

Santos Merino received the PhD degree in Solid State Physics from the Basque Country University, Spain, in 1997. Since then, he has been a Researcher at IK4-Tekniker. He is currently the Head of Micro and Nanofabrication Unit at IK4-Tekniker, developing most of the activity in biosensors and tissue engineering in Health, as well as nanofabrication-based processes for photonic applications.

María A. Díaz-García received the Ph.D. in Physics in 1995 at the Autonomus University of Madrid, Spain. She was part of the pioneer group of Prof. Heeger (Nobel Prize in Chemistry 2000), at the Univ. of California in Santa Barbara, USA, which discovered stimulated emission in semiconducting polymers in 1996. She joined the faculty of the University of Alicante in 2001, where she founded the “Organic Electronics and Photonics” group, which leads since then. She was appointed full professor in 2010. Her latest research focusses on organic optoelectronic materials and devices, with major emphasis on organic lasers.